

TRANSVERSE PHASE-SPACE BEAM TOMOGRAPHY AT PSI AND SNS PROTON ACCELERATORS*

D. Reggiani[#], M. Seidel, PSI, 5232 Villigen, Switzerland
C.K. Allen, ORNL, Oak Ridge, TN 37831, U.S.A.

Abstract

Operation and upgrade of very intense proton beam accelerators like the PSI facility and the neutron spallation source (SNS) at ORNL is typically constrained by potentially large machine activation. Besides the standard beam diagnostics, beam tomography techniques provide a reconstruction of the beam transverse phase space distribution, giving insights to potential loss sources like irregular tails or halos. Unlike more conventional measurement approaches (pepper pot, slits) beam tomography is a non destructive method that can be performed at high energies and, virtually, at any beam location. Results from the application of the Maximum Entropy Tomography (MENT) algorithm [1] to different beam sections at PSI and SNS are shown. In these reconstructions the effect of non-linear forces is made visible in a way not otherwise available through wire scanners alone. These measurements represent a first step towards the design of a beam tomography implementation that can be smoothly employed as a reliable diagnostic tool.

The principle of beam tomography is depicted in Fig. 1. The plot on the left side represents the unknown beam transverse phase-space distribution at the reference position $z = z_0$. Beam profile monitors acquire projections of the phase-space onto the x coordinate at different locations (middle plots). These projections are related to the beam distribution at $z = z_0$ through linear transport matrices accounting for drift space and/or quadrupole magnets. In beam tomography the profile data are employed by a mathematical algorithm in order to reconstruct the two-dimensional beam density distribution (right plot).

Contrary to the case of medical imaging, in beam tomography, due to the very limited number of available projections, the solution of the problem can only be made unique by requiring additional conditions. For the reconstructions presented here the well established MENT approach was employed. Of all possible distribution functions, this algorithm chooses the most probable one, namely the distribution having the maximum entropy. A detailed description of MENT is given in [1] while its first application to beam tomography is described in [2].

INTRODUCTION

The goal of phase-space beam tomography is to reconstruct the phase-space beam density distribution starting from projection data acquired by means of profile monitors. Due to its capability of unveiling the structure of beam tails and halo, the tomography technique can be a very powerful tool for all those accelerator facilities where it is mandatory to keep even tiny beam losses under control.

BEAM TOMOGRAPHY AT PSI

The PSI proton accelerator [3] is a facility generating a continuous wave 590 MeV kinetic energy and, presently, 1.3 MW average power beam and furnished with two graphite meson production targets as well as a neutron spallation target. An overview of the complex is given in Fig. 2.

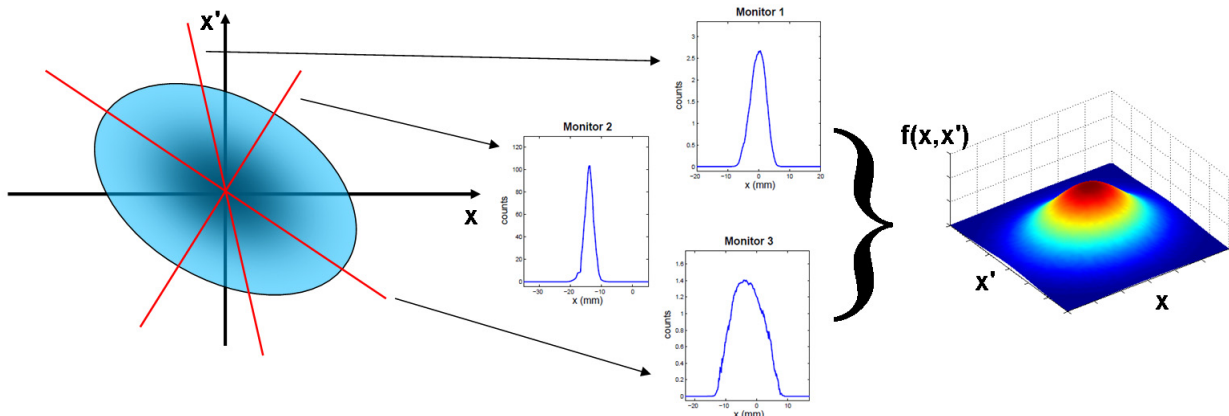


Figure 1: Schematic visualization of the principle of phase-space beam tomography. The coordinates (x, x') refer to the horizontal plane while (y, y') are used for the vertical one.

*SNS is managed by UT-Battelle, LLC, under contract DE-AC05-00OR22725 for the U.S. Department of Energy

[#]Corresponding author (davide.reggiani@psi.ch)

PSI Proton Accelerator Complex

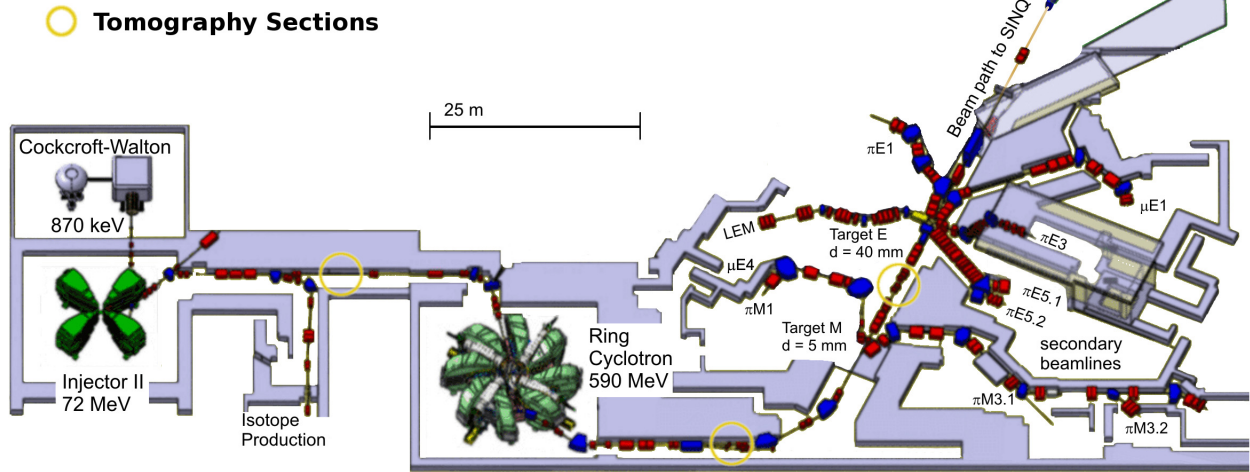


Figure 2: Overview of the PSI high intensity proton accelerator complex. The beam tomography sections are highlighted by yellow circles. The beam envelopes and the location of the relevant beam profile monitors are shown in Fig. 3.

At PSI proton accelerator beam tomography was first implemented almost thirty years ago by W. Joho and U. Rohrer [4] when the beam intensity was about 20 times lower than now. The original MENT code was modified in order to account for the presence of quadrupole magnets between profile monitors, thus allowing to apply a larger number of projection views. Moreover, at that time a drift section of the 72 MeV transfer line between the injector and the main cyclotron was furnished with five beam profile monitor pairs placed at the location of a double waist, making therefore this beam line particularly suitable for beam tomography.

Recently, the PSI version of the MENT code has been employed for new tomography measurements performed at a beam current of 2.2 mA in the 72 MeV transfer line between the injector and the ring cyclotron as well as at two locations of the 590 MeV proton channel: between

the cyclotron extraction and the first meson production target (target M, 5 mm thick), employing up to six beam profile monitor pairs partially alternated by quadrupole magnets, and between the two meson production targets, where three profile monitors are nicely located over a double beam waist. In Fig. 3 the envelopes of the beam sections where tomographic reconstructions have been performed are displayed along with the locations of the beam profile monitors employed for the measurements.

Fig. 4 shows the phase-space reconstruction of the 72 MeV beam. In the five top graphs, the beam profile projection data are plotted (red circles) along with the back-projections from the reconstructed phase-space (blue lines). The location of monitor MPX19 has been chosen as the reference position ($z = 0$). The very good agreement between data and back-projections demonstrates the reliability of the reconstruction.

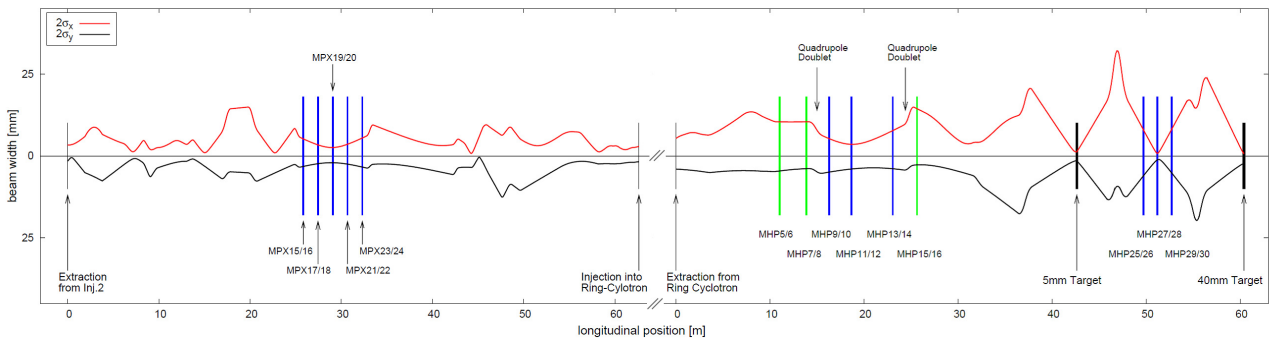


Figure 3: Horizontal and vertical envelopes of the PSI 72 MeV (left) and 590 MeV (right) beam. The larger vertical bars represent the beam profile monitors employed for beam tomography. Blue bars indicates profile monitors located within a drift.

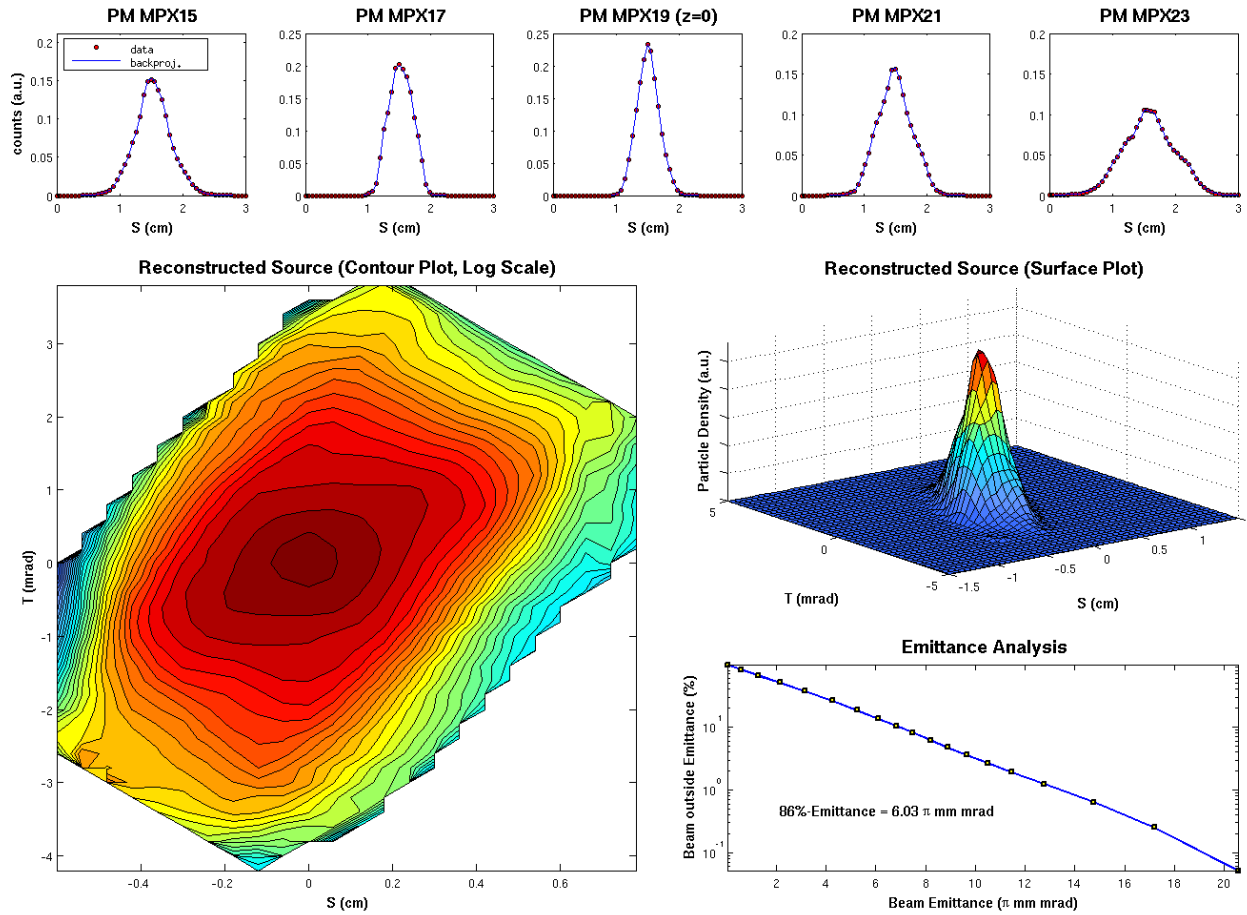


Figure 4: MENT reconstruction of the horizontal phase-space density distribution of the 72 MeV, 2.2 mA proton beam located in the injection line of the PSI cyclotron complex. The MENT variables (S,T) represent the phase-space coordinates (x,x'). A description of the plots is given in the text

Iso-contours of the reconstructed source are plotted in logarithmic scale in order to enhance the visualisation of tails and halo. A linear scale is otherwise employed for the surface plot. Neither plot shows any significant evidence of tails or halo. In the lower-right graph the calculated beam emittance ϵ associated to iso-contours is plotted against the number of beam particles falling outside the emittance itself. This quantity can also be expressed in terms of the action J, where $\epsilon = \langle J \rangle$. The particle density n of a Gaussian distributed beam is an exponential function of J:

$$n(J) = 1 - e^{-J/\epsilon_{rms}}$$

Therefore, the portion of beam falling outside the emittance, $1 - n(J)$, is a decreasing exponential function of J or, in logarithmic scale, a decreasing straight line. In such a plot, non-Gaussian beam distribution caused by tails or collimation can be easily identified by deviations from the linear behaviour in the direction of larger or smaller emittance values respectively. This concept is depicted in Fig. 5. Excluding the very last point, the linearity featured by the emittance analysis of this

reconstruction confirms the absence of substantial beam tails. On the contrary, tails are clearly visible in the reconstructions obtained in the 590 Mev beam section, in particular downstream of the 5 mm thick Target M.

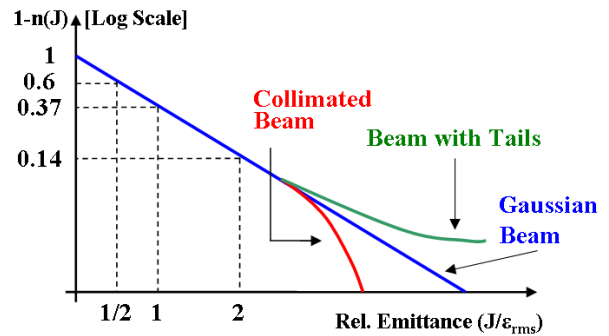


Figure 5: In a Gaussian distributed beam, the number of particles falling outside the beam emittance, $1 - n(J)$, where J is the action variable, is a decreasing exponential function of the beam emittance (blue line). On a logarithmic scale, deviations due to tails or collimation are thus immediately recognizable (red and green lines).

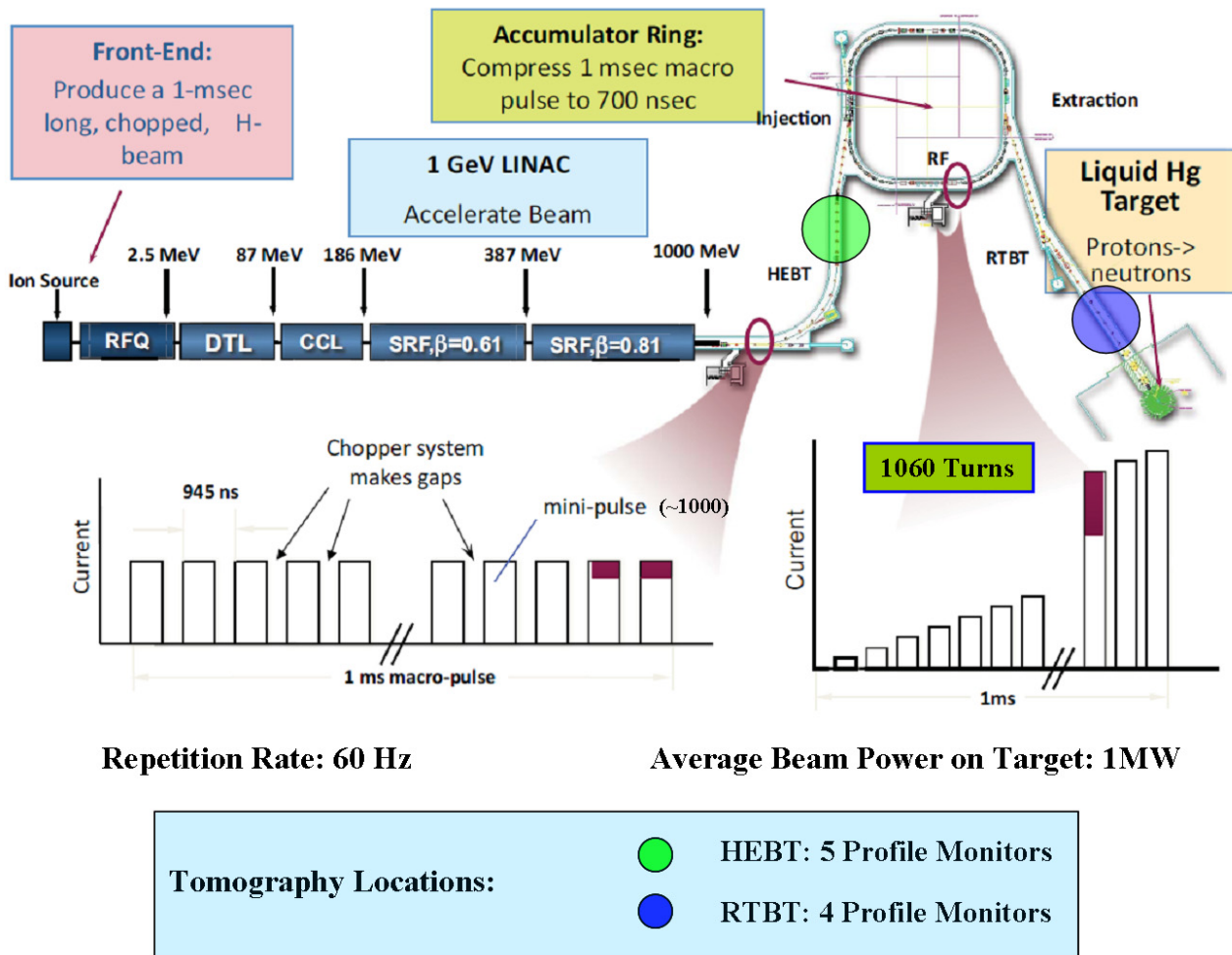


Figure 6: Overview of the SNS accelerator complex. Tomography reconstructions have been performed in two straight sections upstream of the accumulator ring (HTBT) and in front of the spallation target (RTBT) respectively.

BEAM TOMOGRAPHY AT SNS

The SNS facility combines a 1 GeV linac and an accumulator ring in order to produce a 1 MW pulsed proton beam scattering on a liquid mercury neutron spallation target. A detailed description of the SNS accelerator can be found in [5].

Phase-space reconstructions using MENT have been performed at two different locations, both with 1 GeV beam energy: the HEBT1 section, situated between the linac and the accumulator ring, and the RTBT transfer line, upstream of the spallation target. Fig. 7 shows the reconstruction of the HEBT1 beam. The five employed profile monitors are located in the drift regions of a periodic quadrupole lattice. Also in this case, there is very good agreement between data and back-projections. The reconstructed source reveals a clear separation between a sharp core and a beam halo provided with spiral tails. The linearity region of the emittance plot is limited to the region between 0 and $0.5 \pi \cdot \text{mm} \cdot \text{mrad}$, (corresponding to

roughly 50% of the beam). The emittance grows then much faster up to $1.5 \pi \cdot \text{mm} \cdot \text{mrad}$ where a new linear region starts and, finally, for emittance values larger than $3.5 \pi \cdot \text{mm} \cdot \text{mrad}$ a cut-off region appears.

The reconstruction of the beam in the RTBT section, placed between the ring extraction and the spallation target, reveals how the phase-space painting system employed at the accumulator ring injection produces an almost flat transverse phase distribution.

CONCLUSION

A collaboration between PSI and SNS has been established with the goal of implementing beam tomography as a versatile and user-friendly diagnostic tool. First results obtained employing the MENT algorithm delivered very interesting results. The most appropriate technique will be chosen after testing other tomography approaches in the near future.

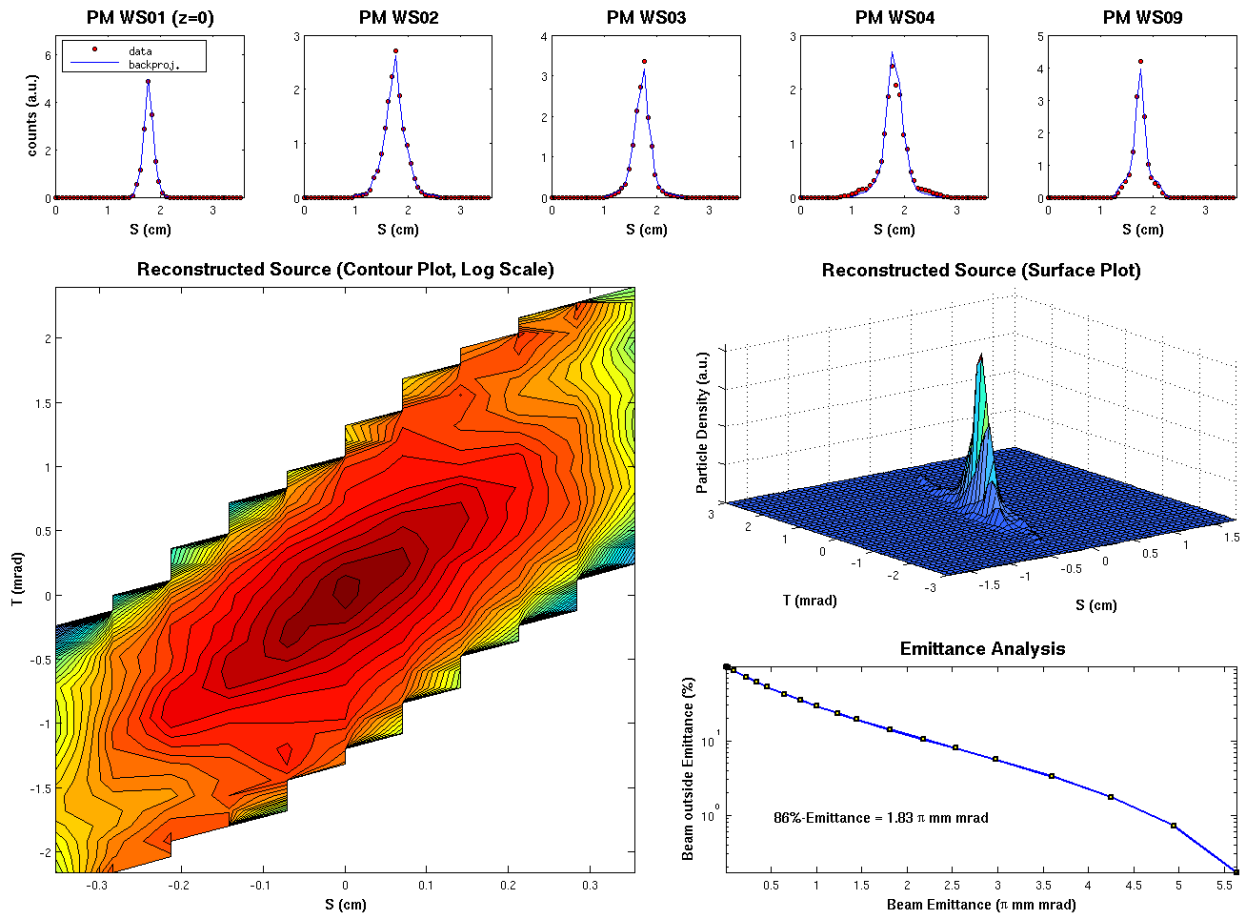


Figure 7: MENT reconstruction of the horizontal phase-space density distribution of the 1 GeV proton beam located in the HEBT1 section of the SNS accelerator, before injection into the accumulator ring. The results are commented in the text.

REFERENCES

- [1] G. Minerbo, MENT: A Maximum Entropy Algorithm for Reconstructing a Source from Projection Data, Computer Graphics and Image Processing 10 (1979) p. 48 – 68.
- [2] C.T. Mottershead, Maximum Entropy Beam Diagnostic Tomography, IEEE Transactions on Nuclear Science, Vol. NS-32, No. 5, October 1985, p. 1970-1972 .
- [3] M. Seidel et al., Production of a 1.3 MW Proton Beam at PSI, Proceedings of IPAC10, p. 1309-1313.
- [4] U. Rohrer, Maximum Entropy Beam Tomography, PSI, <http://pc102.psi.ch/ment.htm>
- [5] N. Holtkamp, The SNS Linac and Storage Ring: Challenges and Progress Towards Meeting Them, Proceedings of EPAC 2002, p. 164-168.